Article

The M-basis Functions and Their Application

Mehran Emadi Andani *

Posted Date: 13 February 2023

doi: 10.20944/preprints202302.0208.v1

Keywords: M-basis function; Fourier basis function; optimization; minimum jerk

Article

The M-Basis Functions and Their Application

Mehran Emadi Andani

Department of Neurosciences, Biomedicine and Movement Sciences, University of Verona, Verona, Italy; mehran.emadiandani@univr.it

Abstract: A new set of basis functions is presented. The foundation in mathematics is established. To reconstruct a signal, it is compared to the Fourier basis functions. The M-basis functions' potential applications are also presented.

Keywords: M-basis function; Fourier basis function; optimization; minimum jerk

1. Introducing M-basis functions

The M-basis functions of the nth-order are defined as the arguments for optimizing the following objective function:

$$\{M\} = \arg\min\left(\int_0^{t_f}\left(\frac{d^n(\theta(t))}{dt^n}\right)^2 dt\right) \quad (1)$$

Subject to knowing the boundary conditions, i.e., the values of θ and up to the (n-1)th derivative of θ at t = 0 and t = t_f, we will show that the solution to (1) is a linear combination of $2n$ basis functions that we call M-basis functions. First, the third-order (n = 3) is discussed because (1) results in minimum jerk patterns [1–16].

1.1. The third-order M-basis functions (minimum jerk)

As shown in [2], the solution of this problem is a quintic spline, or 5th-order polynomial, which can be described as (2).

$$\theta(t) = A^T X(t) \quad (2)$$

where, t is the time variable, and A and X are the following vectors.

$$A = [a_0 \quad a_1 \quad a_2 \quad a_3 \quad a_4 \quad a_5]^T \quad (3)$$

$$X(t) = [1 \quad t \quad t^2 \quad t^3 \quad t^4 \quad t^5]^T \quad (4)$$

A vector defined by (5) shows the boundary conditions at the initial (t = 0) and final (t = t_f) moments.

$$B^T = [\theta(0) \quad \theta(t_f) \quad \dot{\theta}(0) \quad \dot{\theta}(t_f) \quad \ddot{\theta}(0) \quad \ddot{\theta}(t_f)] \quad (5)$$

where, t_f represents the total time duration, B describes the boundary conditions, and the dot on top of θ indicates the first derivative of θ with respect to time. We can change (5) to (6) using (2).

$$B^T = A^T \underbrace{[X(0) \quad X(t_f) \quad \dot{X}(0) \quad \dot{X}(t_f) \quad \ddot{X}(0) \quad \ddot{X}(t_f)]}_{Q} = A^T Q \quad (6)$$

Preprints (www.preprints.org) | NOT PEER-REVIEWED | Posted: 13 February 2023 doi:10.20944/preprints202302.0208.v1

$$Q = \begin{bmatrix} 1 & 1 & 0 & 0 & 0 & 0 \\ 0 & t_f & 1 & 1 & 0 & 0 \\ 0 & t_f^2 & 0 & 2t_f & 2 & 2 \\ 0 & t_f^3 & 0 & 3t_f^2 & 0 & 6t_f \\ 0 & t_f^4 & 0 & 4t_f^3 & 0 & 12t_f^2 \\ 0 & t_f^5 & 0 & 5t_f^4 & 0 & 20t_f^3 \end{bmatrix}$$

We can write (7) using (2) and (6).

$$\theta(t) = A^T X(t) = \underbrace{A^T Q}_{B^T} Q^{-1} X(t) = B^T Q^{-1} X(t) \qquad (7)$$

$$Q^{-1} = \begin{bmatrix} 1 & 0 & 0 & -10/t_f^3 & 15/t_f^4 & -6/t_f^5 \\ 0 & 0 & 0 & 10/t_f^3 & -15/t_f^4 & 6/t_f^5 \\ 0 & 1 & 0 & -6/t_f^2 & 8/t_f^3 & -3/t_f^4 \\ 0 & 0 & 0 & -4/t_f^2 & 7/t_f^3 & -3/t_f^4 \\ 0 & 0 & 0.5 & -.15/t_f & 1.5/t_f^2 & -0.5/t_f^3 \\ 0 & 0 & 0 & 0.5/t_f & -1/t_f^2 & 0.5/t_f^3 \end{bmatrix} \qquad (8)$$

Using (3) and (7), we can write (8).

$$Q^{-1}X(t) = \begin{bmatrix} 1 & 0 & 0 & -10/t_f^3 & 15/t_f^4 & -6/t_f^5 \\ 0 & 0 & 0 & 10/t_f^3 & -15/t_f^4 & 6/t_f^5 \\ 0 & 1 & 0 & -6/t_f^2 & 8/t_f^3 & -3/t_f^4 \\ 0 & 0 & 0 & -4/t_f^2 & 7/t_f^3 & -3/t_f^4 \\ 0 & 0 & 0.5 & -.15/t_f & 1.5/t_f^2 & -0.5/t_f^3 \\ 0 & 0 & 0 & 0.5/t_f & -1/t_f^2 & 0.5/t_f^3 \end{bmatrix} \begin{bmatrix} 1 \\ t \\ t^2 \\ t^3 \\ t^4 \\ t^5 \end{bmatrix} = \begin{bmatrix} 1 - 10t^3/t_f^3 + 15t^4/t_f^4 - 6t^5/t_f^5 \\ 10t^3/t_f^3 - 15t^4/t_f^4 + 6t^5/t_f^5 \\ t - 6t^3/t_f^2 + 8t^4/t_f^3 - 3t^5/t_f^4 \\ -4t^3/t_f^2 + 7t^4/t_f^3 - 3t^5/t_f^4 \\ 0.5t^2 - 1.5t^3/t_f + 1.5t^4/t_f^2 - 0.5t^5/t_f^3 \\ 0.5t^3/t_f - t^4/t_f^2 + 0.5t^5/t_f^3 \end{bmatrix} \qquad (9)$$

It is possible to convert (9) to (10).

$$Q^{-1}X(t) = TM \qquad (10)$$

where, T and M are defined as follows:

$$T = diag(1,1,t_f,t_f,t_f^2,t_f^2) \qquad (11)$$

$$M(t_n) = T^{-1}Q^{-1}X(t) = \begin{bmatrix} 1 - 10t_n^3 + 15t_n^4 - 6t_n^5 \\ 10t_n^3 - 15t_n^4 + 6t_n^5 \\ t_n - 6t_n^3 + 8t_n^4 - 3t_n^5 \\ -4t_n^3 + 7t_n^4 - 3t_n^5 \\ 0.5t_n^2 - 1.5t_n^3 + 1.5t_n^4 - 0.5t_n^5 \\ 0.5t_n^3 - t_n^4 + 0.5t_n^5 \end{bmatrix} \qquad (12)$$

where, t_n is the normalized time variable, *i.e.*, $t_n = t/t_f$. Each row of the M describes one of the M-basis functions. The M-basis functions are normalized in terms of time and can be calculated simply by using (12). Third-order M-basis functions are illustrated in Figure 1.

Preprints (www.preprints.org) | NOT PEER-REVIEWED | Posted: 13 February 2023 doi:10.20944/preprints202302.0208.v1

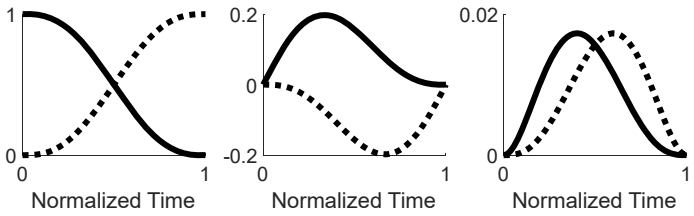

Figure 1. The third-order M-basis functions. Six 3rd-order M-basis functions are illustrated, two in each plot. The third-order M-basis functions are movement elements as derived in [1].

Finally, we can write (13) from (5), (11), and (12).

$$\theta(t) \quad = \quad B^T T M(t_n) \tag{13}$$

Equation (13) shows that the solution of (1) is a linear combination of the M-basis functions scaled by the time duration (T) and boundary conditions (B).

1.2. The n^{th}-order M-basis functions

Similar to [2], it is easy to prove that the solution to (1) is a $(2n-1)^{th}$-order polynomial. Therefore, inspired by what is written above, it is possible to show that the solution of (1) can be described simply by (13) for any order of n.

In this case, X, B, T, and M are as follows:

$$X(t) \quad = \quad [1 \quad t \quad t^2 \quad t^3 \quad \dots \quad t^{2n-1}]^T \tag{14}$$

$$B^T \quad = \quad \left[\theta(0) \quad \theta(t_f) \quad \dot{\theta}(0) \quad \dot{\theta}(t_f) \quad \dots \quad \overbrace{\ddot{\theta}(0)}^{n-1\ dot} \quad \overbrace{\ddot{\theta}(t_f)}^{n-1\ dot}\right] \tag{15}$$

$$T = diag(1,1,t_f,t_f,\dots,t_f^{n-1},t_f^{n-1}) \tag{16}$$

$$M(t_n) \quad = \quad \begin{bmatrix} M_1(t_n) \\ M_2(t_n) \\ . \\ . \\ . \\ M_{2n}(t_n) \end{bmatrix} \tag{17}$$

It should be mentioned that the Q matrix can be created using (18).

$$Q = \left[X(0) \quad X(t_f) \quad \dot{X}(0) \quad \dot{X}(t_f) \quad \dots \quad \overbrace{\ddot{X}(0)}^{n-1\ dot} \quad \overbrace{\ddot{X}(t_f)}^{n-1\ dot}\right] \tag{18}$$

Finally, having Q^{-1} makes it easy to calculate M using (19).

$$M(t_n) = T^{-1}Q^{-1}X(t) \tag{19}$$

Finally, θ can be calculated using (13) with the help of (15), (16), and (17).

Preprints (www.preprints.org) | NOT PEER-REVIEWED | Posted: 13 February 2023 doi:10.20944/preprints202302.0208.v1

1.3. The 4th-order M-basis (minimum snap)

In this case, X, B, T, and M are as follows:

$$X(t) = [1 \quad t \quad t^2 \quad t^3 \quad t^4 \quad t^5 \quad t^6 \quad t^7]^T \tag{20}$$

$$B^T = [\theta(0) \quad \theta(t_f) \quad \dot{\theta}(0) \quad \dot{\theta}(t_f) \quad \ddot{\theta}(0) \quad \ddot{\theta}(t_f) \quad \dddot{\theta}(t_f) \quad \dddot{\theta}(t_f)] \tag{21}$$

$$T = diag(1,1,t_f,t_f,t_f^2,t_f^2,t_f^3,t_f^3) \tag{22}$$

The Q and Q^{-1} can be written as (23) and (24) respectively.

$$Q = \begin{bmatrix} 1 & 1 & 0 & 0 & 0 & 0 & 0 & 0 \\ 0 & t_f & 1 & 1 & 0 & 0 & 0 & 0 \\ 0 & t_f^2 & 0 & 2t_f & 2 & 2 & 0 & 0 \\ 0 & t_f^3 & 0 & 3t_f^2 & 0 & 6t_f & 6 & 6 \\ 0 & t_f^4 & 0 & 4t_f^3 & 0 & 12t_f^2 & 0 & 24t_f \\ 0 & t_f^5 & 0 & 5t_f^4 & 0 & 20t_f^3 & 0 & 60t_f^2 \\ 0 & t_f^6 & 0 & 6t_f^5 & 0 & 30t_f^4 & 0 & 120t_f^3 \\ 0 & t_f^7 & 0 & 7t_f^6 & 0 & 42t_f^5 & 0 & 210t_f^4 \end{bmatrix} \tag{23}$$

$$Q^{-1} = \begin{bmatrix} 1 & 0 & 0 & 0 & -35/t_f^4 & 84/t_f^5 & -70/t_f^6 & 20/t_f^7 \\ 0 & 0 & 0 & 0 & 35/t_f^4 & -84/t_f^5 & 70/t_f^6 & -20/t_f^7 \\ 0 & 1 & 0 & 0 & -20/t_f^3 & 45/t_f^4 & -36/t_f^5 & 10/t_f^6 \\ 0 & 0 & 0 & 0 & -15/t_f^3 & 39/t_f^4 & -34/t_f^5 & 10/t_f^6 \\ 0 & 0 & 0.5 & 0 & -5/t_f^2 & 10/t_f^3 & -7.5/t_f^4 & 2/t_f^5 \\ 0 & 0 & 0 & 0 & 2.5/t_f^2 & -7/t_f^3 & 6.5/t_f^4 & -2/t_f^5 \\ 0 & 0 & 0 & 1/6 & -2/3t & 1/t_f^2 & -2/3t_f^3 & 1/6t_f^4 \\ 0 & 0 & 0 & 0 & -1/6t & 0.5/t_f^2 & -1/2t_f^3 & 1/6t_f^4 \end{bmatrix} \tag{24}$$

Finally, using (20), (22), and (24) as shown below, the M-basis functions can be derived from (19).

$$M(t_n) = \begin{bmatrix} 1 - 35t_n^4 + 84t_n^5 - 70t_n^6 + 20t_n^7 \\ 35t_n^4 - 84t_n^5 + 70t_n^6 - 20t_n^7 \\ t_n - 20t_n^4 + 45t_n^5 - 36t_n^6 + 10t_n^7 \\ -15t_n^4 + 39t_n^5 - 34t_n^6 + 10t_n^7 \\ 0.5t_n^2 - 5t_n^4 + 10t_n^5 - 7.5t_n^6 + 2t_n^7 \\ 2.5t_n^4 - 7t_n^5 + 6.5t_n^6 - 2t_n^7 \\ \frac{1}{6}t_n^3 - \frac{2}{3}t_n^4 + t_n^5 - \frac{2}{3}t_n^6 + \frac{1}{6}t_n^7 \\ -\frac{1}{6}t_n^4 + \frac{1}{2}t_n^5 - \frac{1}{2}t_n^6 + \frac{1}{6}t_n^7 \end{bmatrix} \tag{25}$$

where, t_n is the normalized time variable, *i.e.*, $t_n = t/t_f$. In the end, similarly, θ can be computed by (13) using (21), (22), and (25). Each row of the *M* describes one of the fourth-order M-basis functions. The

Preprints (www.preprints.org) | NOT PEER-REVIEWED | Posted: 13 February 2023 doi:10.20944/preprints202302.0208.v1

M-basis functions from the first to seventh-order are illustrated in Figure 2. The application of the third-order M-basis functions has already been investigated in human movement [1,3–8].

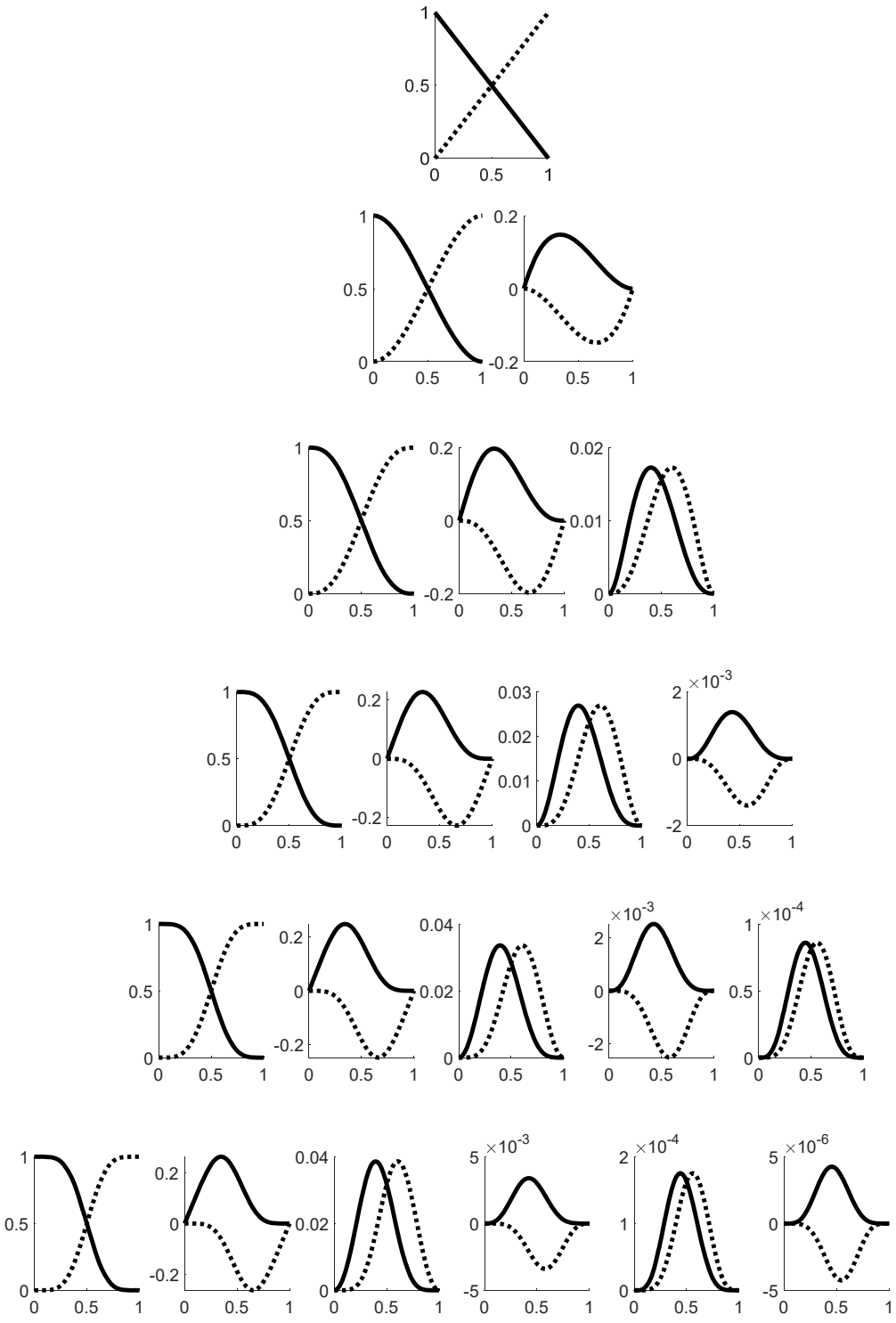

Preprints (www.preprints.org) | NOT PEER-REVIEWED | Posted: 13 February 2023 doi:10.20944/preprints202302.0208.v1

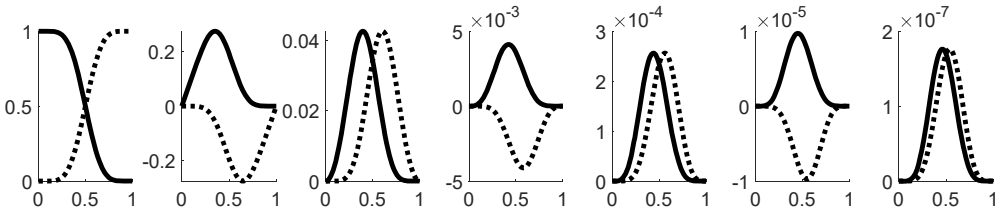

Figure 2. The M-basis functions. The first to seventh rows represent the first to seventh-order M-basis functions, respectively. The horizontal axis is the normalized time. In each window, two M-basis functions are illustrated by solid and dashed lines.

2. The frequency specification of the M-basis functions

According to the definition of the objective function, i.e., equation (1), it can be imagined that the M-basis functions are the low-frequency signals. Considering t_f = 1 sec, the Fourier transforms of the M-basis functions from the first to seventh orders are calculated. It should be added that the two M-basis functions shown in the same window in Figure 2 have the same absolute Fourier transforms. The cutoff frequencies of the M-basis functions for various orders are depicted in Figure 3.

It should be mentioned that the shorter the t_f, the higher the cutoff frequency, and vice versa. It is proportional to the length of time, so the cutoff frequency for a t_f of 0.5 sec is twice that of 1 sec. It means that for the shorter time length, the bandwidth of the M-basis functions is higher. The bandwidth of the M-basis functions, on the other hand, is lower for longer time lengths due to their low-frequency nature.

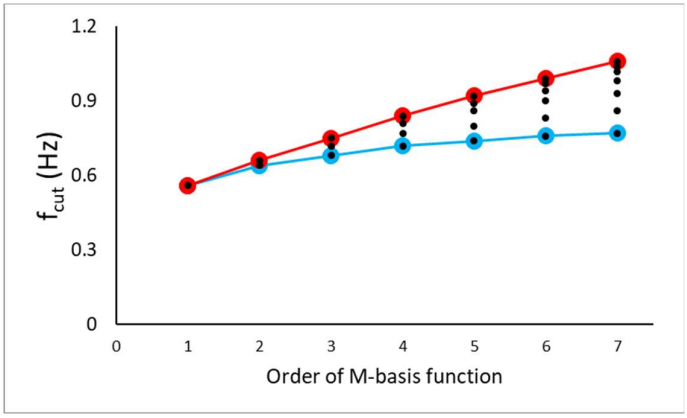

Figure 3. The cutoff frequency. Black circles represent the first- to seventh-order M-basis functions' cutoff frequencies. For the first-order, there are two M-basis functions with the same absolute Fourier transform and therefore the same cutoff frequency. Similarly, there are n cutoff frequencies for the nth-order M-basis functions. The lowest and highest values of the cutoff frequencies are highlighted by blue and red lines, respectively.

3. The applications of the M-basis function

3.1. Human movements

As shown in [1–8], one of the applications of the third-order M-basis functions is in human motor planning. Moreover, it can also be applied to humanoid robots [3,6,7].

3.2. Slow signals

With almost the same number of basis functions, the error of reconstructing a signal using the Fourier basis functions and the M-basis functions is compared. The original signal (Y) is created with

Preprints (www.preprints.org) | NOT PEER-REVIEWED | Posted: 13 February 2023 doi:10.20944/preprints202302.0208.v1

a duration of 1 sec and a sampling frequency of 100 Hz. The results show that a signal with low-frequency information can be represented better by a linear combination of M-basis functions than by Fourier-based functions. Different examples are depicted in Table 1 to show the performance of M-basis functions compared to the Fourier transform. Because the signal has a time length of one second and the resolution of the Fourier basis functions is 1 Hz, the Fourier basis function produces better results for pure sinusoidal signals with integer frequency. For the non-integer frequencies, the Fourier basis functions are not efficient to reconstruct the original signal; however, the M-basis functions can reconstruct these kinds of signals with a limited number of basis functions. For signals with a wider frequency range, the order of the M-basis functions should obviously be higher to reconstruct the signal at higher frequencies, as seen in Fig. 3.

Table 1. The number of basis functions of the Fourier and M transforms needed to reconstruct the signal with a maximum error of 5% is depicted in different cases. Different cases were considered as examples to show the effect of the integer and non-integer values of frequency. The duration of the signal is set at 1 sec (t_f = 1 sec), and the sampling frequency is set at 100 Hz. Since the duration of the signal is 1 sec, the resolution of the Fourier transform is 1 Hz. That is why, in these cases, the number of Fourier basis functions will be increased to compensate for the lack of frequency resolution. The variability in the number of basis functions in the Fourier transform is huge; instead, it is more robust in the M transform. For the signals including non-integer frequencies, the results of M-basis functions are much better, i.e., it needs a much smaller number of basis functions to represent the original data with less than 5% error. In those cases, even with more than 51 of the Fourier basis functions, the represented data had more than 15% error.

Original signal	The number of basis functions needed to reconstruct the original signal with an error rate under 5%	
	Fourier-basis	M-basis
cos(2π×t)	3	8
sin(2π×t)	3	8
cos(2π×2t)	5	14
sin(2π×2t)	5	14
sin(2π×t) + sin(2π×2t)	5	14
2sin(2π×t) + sin(2π×2t)	5	14
cos(2π×0.5t)	>51	4
cos(2π×0.53t)	>51	6
cos(2π ×0.53t - π/8)	>51	6
cos(2π×1.38t)	>51	12
cos(2π×1.38t + π/12)	>51	12
cos(2π×1.38t + π/12) + cos(2π ×0.53t - π/8)	>51	10
cos(2π×1.38t + π/12) + cos(2π ×0.53t - π/8) + cos(2π ×0.17t + π/3)	>51	10

$\sin(2\pi \times t) + \cos(2\pi \times 1.38t + \pi/12) + \cos(2\pi \times 0.53t - \pi/8) + \cos(2\pi \times 0.17t + \pi/3)$	>51	10
$\sin(2\pi \times t) + \sin(2\pi \times 2t) + \cos(2\pi \times 1.38t + \pi/12) + \cos(2\pi \times 0.53t - \pi/8) + \cos(2\pi \times 0.17t + \pi/3)$	>51	14
$\cos(2\pi \times 2.5t)$	>51	18

4. Discussion and conclusion

In this article, I introduced novel M-basis functions. As shown in different examples, representing a signal by M-basis functions can preserve the frequency nature of the signal, especially if the time window is short.

As the future work, the combination of the Fourier and M-basis functions can be studied. The M-basis functions can better represent the boundary of the signal than the middle of the signal, while the Fourier basis functions can better represent the middle of the signal because of the Gibbs effect. The M-basis functions can also be applied to estimate the frequency of the single frequency signals with non-integer value.

References

1. Emadi Andani, M., & Bahrami, F. (2012). COMAP: A new computational interpretation of human movement planning level based on coordinated minimum angle jerk policies and six universal movement elements. *Human Movement Science*, *31*(5), 1037–1055. https://doi.org/10.1016/j.humov.2012.01.001
2. http://www.shadmehrlab.org/book/minimum_jerk/minimumjerk.htm
3. Sadeghi, M., Emadi Andani, M., Parnianpour, M., & Fattah, A. (2013). A bio-inspired modular hierarchical structure to plan the sit-to-stand transfer under varying environmental conditions. *Neurocomputing*, *118*, 311–321. https://doi.org/10.1016/j.neucom.2013.03.016
4. Sadeghi, M., Emadi Andani, M., Bahrami, F. et al. Trajectory of human movement during sit to stand: a new modeling approach based on movement decomposition and multi-phase cost function. Exp Brain Res 229, 221–234 (2013). https://doi.org/10.1007/s00221-013-3606-1
5. M. Emadi, F. Bahrami, M. J. Yazdanpanah and A. Patla, "Movement prediction using an MLP without internal feedback," 2004 IEEE International Conference on Systems, Man and Cybernetics (IEEE Cat. No.04CH37583), The Hague, Netherlands, 2004, pp. 5975-5979 vol.6, https://doi.org/10.1109/ICSMC.2004.1401151
6. Sadeghi, M., Emadi Andani, M., Parnianpour, M., & Fattah, A. (2013b). A bio-inspired modular hierarchical structure to plan the sit-to-stand transfer under varying environmental conditions. Neurocomputing, 118, 311–321. https://doi.org/10.1016/j.neucom.2013.03.016
7. A. KhazeniFard, F. Bahrami, M. E. Andani and M. N. Ahmadabadi, "An energy efficient gait trajectory planning algorithm for a seven linked biped robot using movement elements," 2015 23rd Iranian Conference on Electrical Engineering, Tehran, Iran, 2015, pp. 1006-1011, https://doi.org/10.1109/IranianCEE.2015.7146358
8. N. Fligge, J. McIntyre and P. van der Smagt, "Minimum jerk for human catching movements in 3D," 2012 4th IEEE RAS & EMBS International Conference on Biomedical Robotics and Biomechatronics (BioRob), Rome, Italy, 2012, pp. 581-586, doi: 10.1109/BioRob.2012.6290265.
9. Wang, C., Peng, L., Hou, ZG., Luo, L., Chen, S., Wang, W. (2018). Experimental Validation of Minimum-Jerk Principle in Physical Human-Robot Interaction. In: Cheng, L., Leung, A., Ozawa, S. (eds) Neural Information Processing. ICONIP 2018. Lecture Notes in Computer Science(), vol 11307. Springer, Cham. https://doi.org/10.1007/978-3-030-04239-4_45
10. Slupinski, L., de Lussanet, M.H.E. & Wagner, H. Analyzing the kinematics of hand movements in catching tasks—An online correction analysis of movement toward the target's trajectory. Behav Res 50, 2316–2324 (2018). https://doi.org/10.3758/s13428-017-0995-2
11. Ahmed Asker, Samy F. M. Assal. (2019) A Systematic approach for designing a multi-function sit-to-stand mobility assistive device based on performance optimization. Advanced Robotics 33:2, pages 90-105.
12. Asker, A., Assal, S. F. M., Ding, M., Takamatsu, J., Ogasawara, T., & Mohamed, A. M. (2017). Modeling of natural sit-to-stand movement based on minimum jerk criterion for natural-like assistance and rehabilitation. Advanced Robotics, 31(17), 901–917. https://doi.org/10.1080/01691864.2017.1372214

13. Moullet, E., Roby-Brami, A., & Guigon, E. (2022). What is the nature of motor adaptation to dynamic perturbations? PLOS Computational Biology, 18(8), e1010470. https://doi.org/10.1371/journal.pcbi.1010470
14. Bayle, N., Lempereur, M., Hutin, E., Motavasseli, D., Remy-Neris, O., Gracies, J. M., & Cornec, G. (2023). Comparison of Various Smoothness Metrics for Upper Limb Movements in Middle-Aged Healthy Subjects. Sensors, 23(3), 1158. https://doi.org/10.3390/s23031158
15. Scott T Albert, Alkis M Hadjiosif, Jihoon Jang, Andrew J Zimnik, Demetris S Soteropoulos, Stuart N Baker, Mark M Churchland, John W Krakauer, Reza Shadmehr (2020) Postural control of arm and fingers through integration of movement commands eLife 9:e52507. https://doi.org/10.7554/eLife.52507
16. Emadi Andani, M. (2023) Human movements are shaped by utilizing sensory information: a stochastic optimum model. Preprint, 2023020073. https://doi.org/10.20944/preprints202302.0073.v1